PAPER

NJC
www.rsc.org/njc

Spontaneous deposition of amphiphilic porphyrin films on glass†

Donato Monti,*[a] Mariano Venanzi,[a] Michele Russo,[a] Gianlorenzo Bussetti,[b] Claudio Goletti,[b] Marco Montalti,[c] Nelsi Zaccheroni,[c] Luca Prodi,[c] Roberto Rella,[d] Maria G. Manera,[d] Giovanna Mancini,[e] Corrado Di Natale[f] and Roberto Paolesse*[a]

[a] *Dipartimento di Scienze e Tecnologie Chimiche, Università degli Studi di Roma ''Tor Vergata'', Via della Ricerca Scientifica 1 I-00133, Rome, Italy*
[b] *Dipartimento di Fisica and Unità INFM, Università degli Studi di Roma ''Tor Vergata'', Via della Ricerca Scientifica 1 I-00133, Rome, Italy*
[c] *Dipartimento di Chimica ''G. Ciamician'', Università di Bologna, Via Selmi 2 40126, Bologna, Italy*
[d] *CNR-IMM Sezione di Lecce, Campus Universitario, Università degli Studi di Lecce, Via Arnesano 73100, Lecce, Italy*
[e] *Istituto di Metodologie Chimiche, C.N.R., c/o Dipartimento di Chimica, Università ''La Sapienza'', P.le A. Moro 5 I-00185, Rome, Italy*
[f] *Dipartimento di Ingegneria Elettronica, Università di Roma ''Tor Vergata'', Via della Ricerca Scientifica 1 00133, Rome, Italy*

Received (in Montpellier, France) 8th March 2004, Accepted 26th April 2004
First published as an Advance Article on the web 13th August 2004

Spontaneous deposition of aggregates of a tetraphenylporphyrin derivative, possessing a cationic appended functionality, straightforwardly occurs from aqueous solutions. Combined spectroscopic studies and AFM morphological characterisation reveal that these layered films feature a consistent degree of order. Deposition of the related manganese or cobalt derivatives analogously occurs and the UV-visible spectral pattern of the films dramatically changes upon exposure to vapours of amines or olefins. This aspect can be of great importance for the construction of solid state chemical sensors.

Introduction

The preparation of thin films of porphyrin derivatives is of great interest due to their potentials in materials science[1] and for, among other applications, as optical[2] and chemical sensors,[3] and as solid state synthetic hemoproteins.[4] In the course of our studies, devoted to the preparation of solid state chemical sensors, composed of arrays of quartz crystal microbalances (QCM), we have developed a protocol based on the deposition of self-assembled monolayers (SAMs) of porphyrin diads bearing elements of chirality.[5] These systems present promising features in terms of enantiomeric recognition towards chiral volatile organic compounds. This challenging aspect is remarkably important for the application to real matrices.

One of the most compelling characteristics influencing the properties of porphyrin films is, undoubtedly, the geometry and orientation of the deposited mesostructure. Several strategies can be followed for the preparation of porphyrin layers with controlled features. Construction of SAMs on gold,[6] for example, has led to assemblies with different electrocatalytic properties, depending on the specific orientation of the macrocycles on the gold surfaces.[6c] Langmuir–Blodgett (LB) or Langmuir–Schaefer (LS) techniques[7] have been employed for the fabrication of chiral porphyrin films.[7c,d] Cationic, water-soluble porphyrin derivatives have been shown to adsorb with hydrophilic surfaces by electrostatic interactions, and the orientation of the macrocycles, relative to the substrate surfaces, is dependent on the number and the arrangement of the charged groups.[8] Very recently, it has been reported that the geometry of the absorbed thin layer of porphyrin derivatives can be controlled by depletion interactions.[9] Furthermore, deposition of well-defined porphyrin nanorod aggregates have been reported to occur from acidic solutions of water-soluble porphyrin derivatives[10] or by successive complementary coordination of imidazole to cobalt ion.[11] Peculiar ''wheel-like'' structures have been obtained by controlled evaporation of porphyrin derivative solutions.[12] Porphyrin deposition on quartz, induced by UV irradiation, has also been reported, showing that the photophysical properties of the resulting mesoaggregates can be tuned by changing the central metal ion of the tetrapyrrolic macrocycles.[13] Finally, the self-assembly of giant porphyrin discs has been shown to form astonishing aggregates with well-ordered columnar structure.[14]

In this paper we report on an efficient method of porphyrin layer deposition, by simply dipping a hydrophobic, silanised, glass surface into an aqueous porphyrin solution. Remarkably, the obtained films are characterised by good mechanical stability and, as witnessed by several spectroscopic techniques, by an ordered morphology. Resonance light scattering (RLS) and kinetic experiments provide some information on the plausible mechanism of deposition. Comparisons to the case of deposition of differently functionalised porphyrin derivatives shed some light on the actual nature of the interactions involved. The application of this procedure to some metallo-derivatives may open interesting perspectives for the utilisation of these layered films for gas-sensing applications.

† Electronic supplementary information (ESI) available: detailed kinetic studies and procedures, and aggregation studies on **$1H_2$** and **$2H_2$**. See http://www.rsc.org/suppdata/nj/b4/b403591g/

DOI: 10.1039/b403591g

Results and discussion

As part of our studies on Cytochrome P450 biomimetic systems,[15] we have focused on the aggregation behaviour of several amphiphilised porphyrin derivatives (Chart 1) such as [5-{4-(3-trimethylammonium)propyloxyphenyl}-10,15,20-triphenylporphyrin] chloride (**1H$_2$**), manganese(III) [5-{4-(3-trimethylammonium)propyloxyphenyl}-10,15,20-triphenylporphyrinyl] dichloride (**1MnCl**), cobalt(II) [5-{4-(3-trimethylammonium)propyloxyphenyl}-10,15,20-triphenylporphyrinyl] chloride (**1Co**), 2-[2-(2-(4-(10,15,20-triphenyl-5-porphyrinyl)-phenoxy)ethoxy)ethoxy]ethanol (**2H$_2$**), and [5-(4-carboxyphenyl)-10,15,20-triphenylporphyrin] (**3H$_2$**) in aqueous solvent mixtures. UV-visible spectra of **1H$_2$** aqueous solutions (μM concentration) showed the formation of porphyrin aggregates on gradually going from pure ethanol to a water–ethanol (9 : 1 v/v) solvent mixture. Moreover, the presence of several well-defined isosbestic points indicates the occurrence of a controlled self-assembly process toward the formation of a narrow distribution of species.[16] UV-visible spectral changes and concomitant molecular deposition occurs spontaneously with time, from the aqueous solvent mixture (Figure S1; ESI). Microscope glass slides, with silanised hydrophobic surface, were used as the substrate. Dipping the slides into an aqueous solution of **1H$_2$** (2×10^{-6} to 7.5×10^{-5} M; H_2O–EtOH 9 : 1 v/v) resulted in the deposition of porphyrin aggregates, as evidenced by the typical yellow colouration of the glass surfaces. Complete deposition (UV-vis check of the Soret bands) is achieved in 12–24 h, depending on the concentration of the starting aqueous solutions.

The porphyrin films showed good mechanical stability. Intense rinsing and wipe-drying processes cause no loss of material. Moreover, overnight dipping in absolute ethanol resulted only in a 25–30% decrease of absorption intensity (Soret band). UV-vis spectra (Fig. 1, trace c) of a glass layered **1H$_2$** show a coupled Soret band centred at *ca.* 415 nm, indicating electronic interaction between adjacent layered porphyrin macrocycles[17] with a head-to-tail arrangement.

The extent of deposition depends on the initial concentration of the solution. Similarly, spectra of the final aqueous solutions feature a coupled Soret band, of analogous structure, indicating the presence of interacting chromophores (Fig. 1, trace d). A plot of absorption *vs.* initial porphyrin concentration shows a linear dependence up to *ca.* 2×10^{-5} M (Fig. 1, inset), likely indicating a uniform and regular deposition of layers.[18] On the other hand, a levelling-off effect is observed on further increase

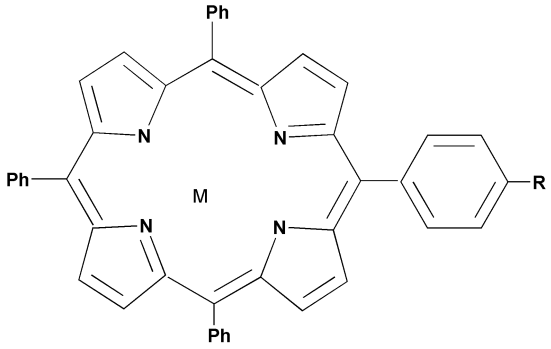

1H$_2$: R = $OCH_2CH_2CH_2NMe_3Cl$; M = 2H

1MnCl: R = $OCH_2CH_2CH_2NMe_3Cl$; M = MnCl

1Co: R = $OCH_2CH_2CH_2NMe_3Cl$; M = Co

2H$_2$: R = $O(CH_2CH_2O)_2CH_2CH_2OH$; M = 2H

3**H$_2$:** R = CO_2H; M = 2H

Chart 1

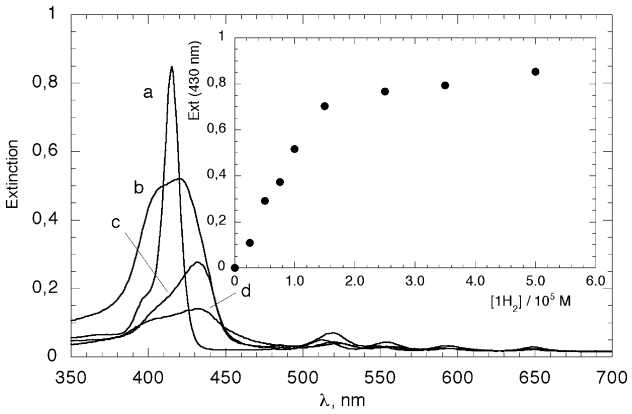

Fig. 1 UV-vis spectra of **1H$_2$** (5.0×10^{-6} M): (a) in EtOH; (b) in H_2O–EtOH (9 : 1 v/v); (c) on glass slide; (d) UV-vis spectrum of **1H$_2$** solution after deposition. Inset: dependence of glass layered porphyrin absorbance (λ 431 nm) at different initial bulk concentrations.

of the starting concentration. This should be essentially due to the formation of higher, insoluble aggregates, as indicated by incipient precipitation of some porphyrinic material from the bulk solution.

The atomic force microscopy (AFM) technique was used in order to characterise the porphyrinic films. Typical images are reported in Fig. 2. Interestingly, the AFM picture showed a quite peculiar morphology of the layered aggregates. The wavy appearance can be the result of stratification of regularly oriented porphyrin mesostructures, extending regularly over the whole micrometric scale, of about 500 nm width and 250 nm height. The estimated RMS roughness value, measured in the "canals", is about 1.8 ± 0.1 nm.

This morphology guarantees a high surface/volume ratio and consequently, a high number of absorption sites available for vapour–surface interaction. Deposition on bare glass surfaces (*i.e.*, not silanised) results in a reduced thickness of the films. The related AFM spectra (reported in Figure S2; ESI) reveal a rather porous structure, with average surface roughness and a mean height, calculated on an area of 10 μm × 10 μm, of 4.6 ± 0.4 and 10 ± 1 nm, respectively. The presence of islands of porphyrin aggregates, randomly distributed on the surface, with a bigger height than the rest of the film, is also evident. This different morphology can be correlated to the hydrophobicity of the glass surfaces, as revealed by some experimental evidence. (i) The extent of deposition onto a hydrophilic glass surface is decreased and occurs with random morphology. (ii) Aqueous solutions of porphyrin aggregates of **2H$_2$** and **3H$_2$**, characterised by the presence, respectively, of a neutral or anionic appended functionality (Chart 1), did not result in an appreciable deposition of material onto the glass surface. (iii) The molecular deposition is favoured by an

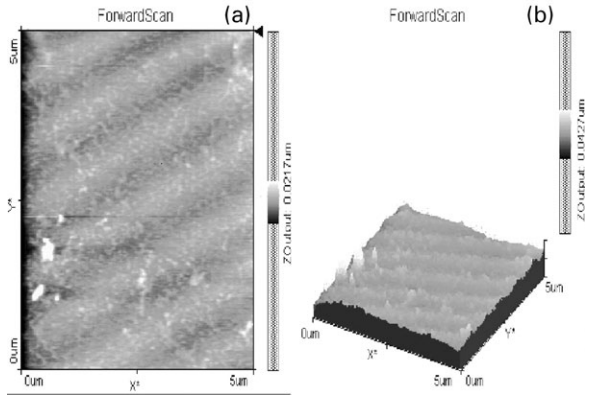

Fig. 2 AFM picture of layered **1H$_2$** (1.0×10^{-5} M): (a) on silanised glass surface and (b) the related three-dimension representation.

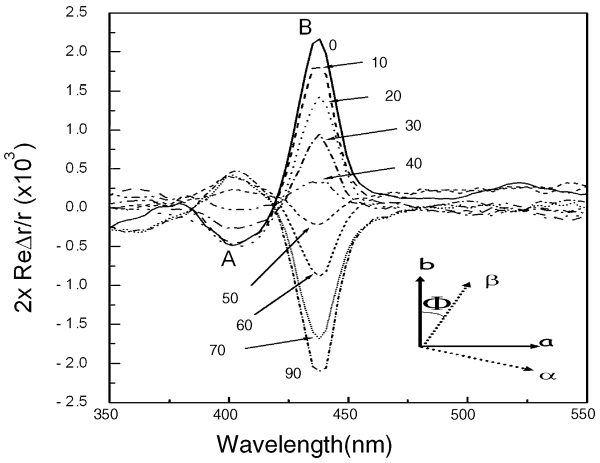

Fig. 3 RAS spectra of $\mathbf{1H_2}$ (5.0×10^{-6} M) on glass at different azimuthal angle Φ (see text). The signal is expressed as $2\mathrm{Re}(\Delta r/r) = \Delta R/R$, where R is the sample reflectance. In the inset, the orientation between the RAS axes a and b and sample axes α and β is sketched.

increase of ionic strength of the solution (*e.g.*, 1×10^{-4} to 0.1 M NaCl; not shown). (iv) Finally, tetrakis(4-methylpyridinium)porphyrin derivative, which does not aggregate within the considered range of concentrations, does not layer onto hydrophobic substrates.‡ All these findings should indicate that the deposition is driven by hydrophobic effects and, noteworthy, occurs spontaneously only in the case of the formation of ordered and uniform aggregates. The occurrence of π-cation interactions would be taken into consideration for the achievement of these structures with ordered morphology.[19] This "*conditio sine qua non*" is witnessed by the fact that neither the neutral $\mathbf{2H_2}$ nor the anionic $\mathbf{3H_2}$ derivatives form regular aggregates, as evidenced by the lack of isosbestic points of their UV-visible spectral changes in water–ethanol mixed solvents.[16c]

In the case of untreated, hydrophilic, glass surfaces, the presence of polar moieties or an ionic charge would be competitive with the noncovalent interactions present in the porphyrin aggregates, resulting in a deposition with a poorly defined morphology.

Reflectance anisotropy spectroscopy (RAS) studies further corroborate this hypothesis. The RAS spectrum of a $\mathbf{1H_2}$ layer (5.0×10^{-6} M) is reported in Fig. 3 for different values of the azimuthal angle Φ, defining the sample rotation around an axis perpendicular to the surface and nearly coincident with the direction of incident light. At $\Phi = 0$, axes a and b of the linearly polarised light coincide with directions α and β, respectively parallel and perpendicular to the rows imaged by AFM in Fig. 2. In this configuration two anisotropy features, with opposite polarisation, are clearly present at $\lambda = 400$ nm (peak A) and $\lambda = 437$ nm (peak B). From studies of porphyrin LB layers,[20] it is known that RAS detects anisotropy features in coincidence with the absorption maxima of the UV-visible absorption spectrum of the sample. In this case, we note that the positions of both A and B peaks are in good agreement with the coupled Soret bands related to the electronic transitions of the porphyrin aggregates (see Fig. 1, trace c). When Φ is changed, the amplitudes of peaks A and B vary, reaching their maximum at $\Phi = 0$.§ However, the overall spectrum lineshape is preserved. The sample exhibits the same behaviour over its whole surface. On the contrary, when RAS experiments are performed on

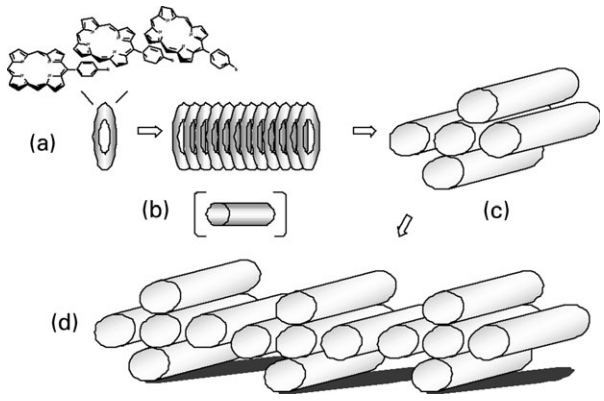

Scheme 1 Hypothesis of the formation of $\mathbf{1H_2}$ supramolecular mesoscopic structures (see text). Some of the porphyrin substituents have been omitted for clarity.

samples of the same porphyrin layered on untreated glass surfaces, the spectra have a different appearance if measured at different azimuthal angles or different positions on the sample surface (see Figure S3; ESI). This effect most probably results from a different degree of local order as well as to the presence of islands of porphyrin aggregates, as shown by AFM studies.

The complexity of aggregation processes, and consequent deposition on solid substrates of related porphyrin systems, hampers a detailed mechanistic investigation. However, some experiments, based on spectroscopic techniques such as combined resonance light scattering (RLS) studies and kinetic experiments (see ESI), as well as the topographic AFM images, may suggest a plausible mechanism of deposition, which has been pictorially reported in Scheme 1.

The injection of aliquots of porphyrin ethanolic stock solution into a water–ethanol mixture (9 : 1 v/v; see Experimental) results in the immediate formation of porphyrin aggregates. Aggregation of water-soluble porphyrin monomers has been reported to be a very fast process, usually completed within the time of mixing.[21] In our case, the rather low solubility of the title porphyrin derivatives in aqueous solvents brought us to the safe assumption that the aggregation process should occur in an even faster step. These porphyrin aggregates, probably with an initial head-to-tail ribbon-like morphology, grow with time to give very large assemblies of supramolecular structures. This hypothesis is corroborated by resonance light scattering studies (RLS). This well-known technique, based on enhancement of the scattering light in the red edge of the Soret band, is strongly dependent on the size of porphyrin aggregates, the electronic coupling among adjacent chromophores, and on their molar extinction coefficient.[22]

It has been reported that the minimum number of interacting chromophores needed to observe the RLS effect is $n \geq 25$ (typically 10^4–10^5 monomer units).[23] Indeed, light scattering experiments on an aqueous solution of $\mathbf{1H_2}$ (5×10^{-6} M, water–ethanol 9 : 1 v/v) show a gradual growth of the RLS signal with time, in the region of the Soret band ($\lambda = 445$ nm), with the intensity approaching a maximum value in about 1 h (Fig. 4). This finding is consistent with the proposed mechanism in which initial single ribbons of porphyrin aggregates (*i.e.*, small ribbons, with $n < 25$ monomer units) rapidly grow and loop themselves to give large ring-shaped porphyrin elements (a), which subsequently associate, by π-π stacking in a fast equilibrium, to form π-stacked columnar structures of mesoscopic size (b) and barrel-shaped forms (c),¶ which eventually self-

‡ It has been reported that the interaction of charged porphyrin derivatives, such as di-, tri-, and tetrakis(4-methylpyridinium)porphyrin, interact with Si–OH or $Si–O^-$ groups of hydrophilic glass surfaces by electrostatic forces (see ref. 14).

§ It has been reported that the absorption spectra of deposited linear porphyrin aggregates, using polarised light, show a clean anisotropy on changing the orientation of the incident light, with respect to the axes of the mesoscopically oriented assembly. See, for example, ref. 11

¶ It can be assumed that these rings, probably of 100–200 nm of diameter, as indicated by AFM, should be formed by aggregation of 500–1000 porphyrin units. It is worth noting that both the UV-vis absorption and emission spectra of films of layered $\mathbf{1H_2}$ are surprisingly similar to those reported for columnar aggregates of ring-shaped architectures of porphyrins (see ref. 14a).

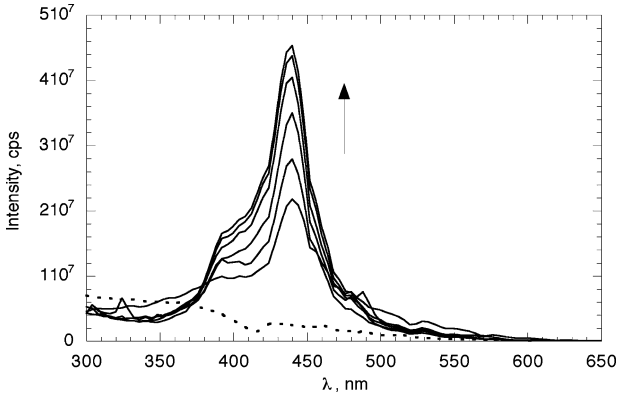

Fig. 4 RLS spectra of $\mathbf{1H_2}$ (5.0×10^{-6} M) taken at 5, 10, 15, 30, 45, 60 min, lowermost to uppermost curves, respectively. Dotted line represents the RLS spectrum of $\mathbf{1H_2}$ in ethanol.

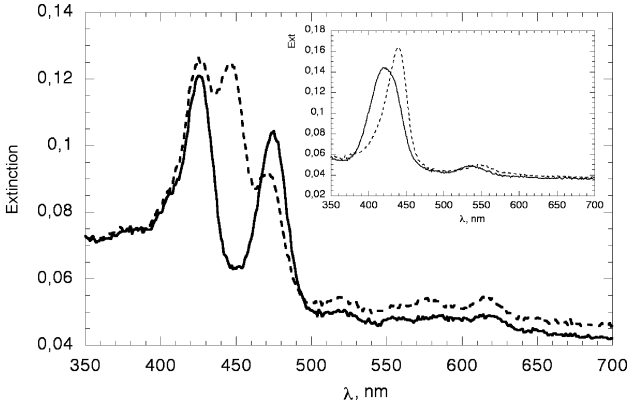

Fig. 5 Absorption spectra of layered **1MnCl** (5×10^{-6} M) in air (solid line) and upon exposition of Et_3N vapours (dotted line). Inset: Absorption spectra of **1Co** (5×10^{-6} M) in air (solid line) and in *R*-(+)-limonene vapour (dotted line).

aggregate in a slow step to form mesostructures (d). These supra-aggregates, once having reached a critical dimension, layer onto the glass substrate collapsing from the solution. On the other hand, ethanol solutions of $\mathbf{1H_2}$ do not features any RLS signals, presenting, instead, a well arising from photon loss in the region of the Soret band due to self-absorption of the monomeric porphyrin species.

Kinetic studies are carried out by means of UV-visible spectroscopy (Soret band, at 430 nm) by following the depletion of porphyrin aggregates from the bulk aqueous solutions (Figure S1, Figure S4 and Table S1; ESI). An apparent first-order reaction rate (k_{app}) is found, from the analysis of the initial part of the kinetics, up to three half times.[24] After that initial period (12–24 h), the extinction of the bulk solution reaches a plateau, indicating the presence of an equilibrium. It is worth noting that the equilibrium solution (*e.g.*, trace d, Fig. 1) presents a spectral pattern similar to that observed in the solid phase (see, for example, the lowermost trace of Figure S1; ESI). This should rule out the possibility that the layered structures are formed directly on the glass surface in a stepwise fashion. Moreover, analogous experiments, carried out by monitoring the film growth on the glass substrates, gave similar values, within experimental errors, of the deposition rate constants on the glass substrate (see Figure S5, and Table S1 in ESI). These findings corroborate the hypothesis given by the proposed mechanism.‖

Moreover, films of $\mathbf{1H_2}$ on glass show a fluorescence signal ($\lambda_{exc} = 430$ nm, $\lambda_{em} = 658$; 720 nm). The excitation spectrum, at $\lambda = 658$ nm, is virtually superimposable on the absorption spectrum. An identical effect arises from the excitation at 415 nm. An analogous result is obtained by excitation at 720 nm. This is not an unexpected result, in that the considered bands originate from a solid-state excitonic coupling of electronically interacting chromophores, and not from different chemical species (Figure S6, in ESI). The excited state decay features two lifetimes of 10.0 and 0.5 ns, the latter being the predominant one, typical of electronically interacting macrocycles.[16a,25]

Analogous studies reveal that deposition spontaneously occurs also in the case of the corresponding Mn(III) and Co(II) metalloderivatives. These porphyrin films are characterised by the presence of broadened Soret and Q bands, and in the case of **1MnCl**, by an intense ligand-to-metal charge-transfer band (LMCT) at *ca.* 475 nm. Furthermore, by exposing a glass film of **1MnCl** to vapours of triethylamine, for example, a dramatic change of the spectral pattern, in terms of LMCT band hypochromicity and red shift of the Soret band, occurs (Fig. 5), as a consequence of metal coordination. Subsequent flushing with an N_2 stream restores the initial UV-visible features. Analogously, significant spectral changes are featured by a **1Co** film upon exposure to alkene vapours such as, for example, limonene (Fig. 5, Inset). The evident sharpening of the Soret band is a consequence of a decrease of the electronic interaction (reduced π-π stacking) among the chromophores, indicating that the host molecules are included within the layered porphyrin macrocycles, as a consequence of concomitant metal–olefin coordination and π-π interactions. The same interactions have been reported to be operative in the case of self-assembled monolayers of chiral porphyrin diads.[5]

Conclusions

In summary, this work presents a facile and straightforward way to obtain porphyrin films with an ordered morphology. Related studies carried out on metalloderivatives showed the possibility to build up a simple system for the detection of organic volatiles. Application of the reported protocol to chiral porphyrin derivatives, for the preparation of enantioselective sensors, is currently under investigation in our laboratories.

Experimental

General

UV-visible spectra were performed on a Perkin Elmer λ18 Spectrophotometer. All solvents used were of highest degree of purity and used as received. Porphyrin solutions for spectroscopic studies have been prepared by using solvents of spectroscopic grade. Milli-Q, Millipore, previously doubly distilled water, was used for the preparation of porphyrin aqueous solutions.

Synthesis of porphyrin derivatives

Porphyrin derivatives $\mathbf{1H_2}$, **1MnCl**, $\mathbf{2H_2}$, and $\mathbf{3H_2}$ were prepared according to procedures previously reported.[15]

Cobalt(II) [5-{4-(3-trimethylammonium)propyloxyphenyl}-10,15, 20-triphenylporphyrinyl] chloride (1Co). This compound was prepared as follows: in a 50 mL round bottomed flask, 60 mg of porphyrin $\mathbf{1H_2}$ (0.08 mmol) were dissolved in 25 mL of dry $CHCl_3$. To the resulting solution, 3 mL of a saturated methanolic solution of cobalt(II) acetate were added. The reaction

‖ The obtained rate constant values, k_{app}, follow a nonlinear, Langmuir-type dependence on the initial concentration of $\mathbf{1H_2}$ (see Figure S4; ESI), with the deposition rate tending toward a limiting value, on increasing the initial porphyrin bulk concentration, as expected for a *monomolecular-like* (*i.e.* well-defined noncovalent suprastructures) deposition onto a surface. An alternative mechanism would regard the "barrel-like" structure deposition as the slow, rate determining step, or a parallel process. This hypothesis, however, would be rather speculative at this stage. More detailed kinetic studies will be carried out and the results will be reported elsewhere.

mixture was stirred under a N_2 atmosphere at reflux temperature until the metallation was completed (*ca.* 3 h, UV-visible check). The mixture was then cooled to room temperature, diluted with $CHCl_3$ to 50 mL, washed with brine (3×100 mL), and dried. The solvent was removed under reduced pressure and the brownish residue crystallised from CH_2Cl_2–hexane to give 40 mg of pure **1Co** (0.05 mmol, 60% yield) as a reddish-brown microcrystalline solid. UV-vis ($CHCl_3$): λ_{max}/nm (log ε) 440 (4.8), 552 (3.2), 592 (3.0). FAB-MS (NBA) m/z: 786 $[M - HCl]^+$; 727 $[M - ClNMe_3]^+$; 670 $[M - Cl - OCH_2CH_2CH_2NMe_3]^+$.

Preparation of samples

Microscope glass slides (Forlab®; Carlo Erba, cut into 25×8 mm^2 pieces) were used as film substrates. (i) The slides were immersed into a mixture of concentrated NH_4OH and 30% H_2O_2 (30 min) then thoroughly rinsed with water (Milli-Q, Millipore) and dried (120 °C). The slides were then immersed in hexamethyldisiloxane (overnight), washed with toluene and dried. (ii) Substrate depositions were achieved by dipping the glass slides into the appropriate volume of freshly prepared porphyrin solution (2.0×10^{-6} to 5.0×10^{-5} M; H_2O–EtOH 9 : 1 v/v; 48 h; 35 °C). The slides were washed (H_2O–EtOH 9 : 1 v/v) and dried (N_2 stream, 40 °C). Reproducibility of the layer thickness is within 5–10% (UV-visible spectroscopy check of the absorption maxima). Deposition on raw, untreated glass slides gave less reproducible results.

AFM studies

The surface topography of porphyrin films was investigated in air by contact mode atomic force microscopy (AFM) using low tip force. The observations were performed by using an EXPLORER-VEECO system with a Si_3N_4 pyramidal tip having a curvature radius lower than 50 nm. For each sample, different images were recorded from different positions in order to check the lateral uniformity of the films. This allowed us to calculate the value of the root mean square of the surface average roughness, RMS, of the films.

Reflectance anisotropy spectroscopy (RAS) studies

RAS measures the reflectivity difference between two perpendicular directions of the sample, thereafter called *a* and *b*. The direction of polarisation of the light electric field is modulated, at a characteristic frequency f_0, along *a* and *b* by a home-made photo elastic modulator (PEM) acting as a half-wavelength retarder.[26a] The results are given in terms of the ratio between the variation of the sample reflectivity (Δr) and the average reflectivity (r): $\Delta r/r = 2(r_a - r_b)/(r_a + r_b)$. $(\Delta r/r)$ is a complex quantity, whose real and imaginary parts exhibit different modulation frequencies, respectively f_0 and $f_0/2$.[26b] The two components can be measured simultaneously using a lock-in amplifier. Only the real part of $\Delta r/r$, which represents the anisotropy of the reflected intensity, is considered in this work.[26b] The RAS apparatus employed in our studies, suitable to performing optical measurements in the range 200–800 nm (1.5–6 eV), has been assembled in our laboratories; a detailed description has been reported elsewhere.[26c]

Fluorescence spectroscopy experiments

Fluorescence and excitation spectra were recorded, at 25 ± 0.5 °C, on a Spex Fluorolog Fluorimeter. Excited state lifetimes were measured on a time-correlated single-photon counting apparatus from Edinburgh Instruments.

Resonance light scattering (RLS) experiments

RLS experiments have been performed on a Spex Fluorolog Fluorimeter. Spectra have been acquired, at 25 ± 0.5 °C, in a "synchronous scan" mode,[23] in which the emission and excitation monochromators are pre-set to identical wavelengths. Solutions have been prepared by injection of the appropriate aliquots of $\mathbf{1H_2}$ stock solutions in ethanol (5–50 μL of mM concentration) in 4 mL of a water–ethanol (9 : 1 v/v) solvent mixture, contained in a 8 mL silanised glass vial. The final concentrations were within the μM range. At scheduled times, aliquots of solutions (3 mL) were taken and transferred into a quartz cuvette (1 cm path) and the RLS spectra acquired.

Acknowledgements

The authors wish to thank MIUR-FIRS "*Sensori Ottici ed Elettroottici per Applicazioni Industriali ed Ambientali*" (Project SAIA-2003) for funding.

References

1 (*a*) J.-H. Chou, H. S. Nalwa, M. E. Kosal, N. A. Rakow and K. S. Suslick, in *The Porphyrin Handbook*, eds. K. M. Kadish, K. M. Smith and R. Guilard, Academic Press, New York, 2000, vol. **6**, ch. 41, p. 43; (*b*) S. Forrest, *Chem. Rev.*, 1997, **97**, 1793; (*c*) C. van Nostrum and R. J. M. Nolte, *Chem. Commun.*, 1996, 2385.
2 M. P. Debreczeny, W. A. Svec and M. R. Wasielewski, *Science*, 1996, **274**, 584.
3 T. Malinski, in *The Porphyrin Handbook*, eds. K. M. Kadish, K. M. Smith, R. Guilard, Academic Press, New York, 2000, vol. **6**, ch. 44, p. 231.
4 D. L. Pilloud, F. Rabanal, B. R. Gibney, R. S. Farid, P. L. Dutton and C. C. Moser, *J. Phys. Chem. B*, 1998, **102**, 1926.
5 R. Paolesse, D. Monti, L. La Monica, M. Venanzi, A. Froiio, S. Nardis, C. Di Natale, E. Martinelli and A. D'Amico, *Chem.-Eur. J.*, 2002, **8**, 2476.
6 (*a*) D. T. Gryko, C. Clausen and J. S. Lindsey, *J. Org. Chem.*, 1999, **64**, 8635; (*b*) Z. Zhang, S. Hou, Z. Zhu and Z. Liu, *Langmuir*, 2000, **16**, 537; (*c*) Z. Zhang, R. Hu and Z. Liu, *Langmuir*, 2000, **16**, 1158.
7 (*a*) A. Ulman,n *An Introduction of Ultrathin Organic Films, from Langmuir–Blodgett Films to Self-Assembly*, Academic Press, San Diego, CA, 1991; (*b*) J. M. Kroon, E. J. R. Sudhölter, A. P. H. J. Schenning and R. J. M. Nolte, *Langmuir*, 1995, **11**, 214; (*c*) L. Zhang, Q. Lu and M. Liu, *J. Phys. Chem. B*, 2003, **107**, 2565; (*d*) L. Zhang, J. Yuan and M. Liu, *J. Phys. Chem. B*, 2003, **107**, 12 768.
8 (*a*) T. J. Savenije, C. H. M. Marée, F. H. P. M. Habraken, R. B. M. Koehorst and T. J. Schaafsma, *Thin Solid Films*, 1995, **265**, 84; (*b*) J. Wienke, F. J. Kleima, R. B. M. Koehorst and T. J. Schaafsma, *Thin Solid Films*, 1996, **279**, 87.
9 D. Zhou, J. Zhang, L. Li and G. Xue, *J. Am. Chem. Soc.*, 2003, **125**, 11 774.
10 (*a*) A. D. Schwab, D. E. Smith, C. S. Rich, E. R. Young, W. F. Smith and J. C. de Paula, *J. Phys. Chem. B*, 2003, **107**, 11 339; (*b*) R. Rotomskis, R. Augulis, V. Snitka, R. Valiokas and B. Liedberg, *J. Phys. Chem.*, 2004, **108**, 2833.
11 C. Ikeda, E. Fujiwara, A. Satake and Y. Kobuke, *Chem. Commun.*, 2003, 616.
12 L. Latterini, R. Blossey, J. Hofkens, P. Vanoppen, F. C. De Schryver, A. E. Rowan and R. J. M. Nolte, *Langmuir*, 1999, **15**, 3582 and references therein.
13 L. Monsù Scolaro, A. Romeo, M. A. Castriciano, G. De Luca, S. Patanè and N. Micali, *J. Am. Chem. Soc.*, 2003, **125**, 2040.
14 (*a*) M. C. Lensen, K. Takazawa, J. A. A. W. Elemans, C. R. L. P. N. Jeuskens, P. C. M. Christianen, J. C. Maan, A. E. Rowan and R. J. M. Nolte, *Chem.-Eur. J.*, 2004, **10**, 831; (*b*) M. C. Lensen, S. J. T. van Dingenen, J. A. A. W. Elemans, H. P. Dijkstra, G. P. M. van Klink, G. van Koten, J. W. Gerritsen, S. Speller, R. J. M. Nolte and A. E. Nolte, *Chem. Commun*, 2004, 762.
15 (*a*) D. Monti, P. Tagliatesta, G. Mancini and T. Boschi, *Angew. Chem., Int. Ed.*, 1998, **37**, 1131; (*b*) S. Borocci, F. Marotti, G. Mancini, D. Monti and A. Pastorini, *Langmuir*, 2001, **17**, 7198.
16 (*a*) D. Monti, M. Venanzi, V. Cantonetti, S. Borocci and G. Mancini, *Chem. Commun.*, 2002, 774; (*b*) D. Monti, A. Pastorini, M. Venanzi, S. Borocci and G. Mancini, *J. Porphyrins Phthalo-*

cyanines, 2003, **7**, 181; (*c*) D. Monti, V. Cantonetti, M. Venanzi, F. Ceccacci, C. Bombelli and G. Mancini, *Chem. Commun*, 2004, 972.
17 J. M. Ribó, J. M. Bofill, J. Crusats and R. Rubires, *Chem.-Eur. J.*, 2001, **7**, 2733 and references therein.
18 This has been reported, for example, in the case of electrostatically driven multilayer porphyrin and phthalocyanine film deposition: (*a*) M. A. Castriciano, A. Romeo and L. Monsù Scolaro, *J. Porphyrins Phthalocyanines*, 2002, **6**, 431; (*b*) Y. Sun, C. Sun, Z. Wang, J. Shen, D. Wang and T. Li, *Chem. Commun*., 1996, 2379.
19 These non-covalent interactions are known to play a fundamental role in supramolecular host-guest recognition, as well as in important biological systems. For an overview see, for example: J. C. Ma and D. A. Daugherty, *Chem. Rev*., 1997, **97**, 1303.
20 (*a*) C. Di Natale, C. Goletti, F. Della Sala, M. Drago, P. Chiaradia, R. Paolesse, P. Lugli and A. D' Amico, *Appl. Phys. Lett*., 2000, **77**, 3164; (*b*) C. Goletti, R. Paolesse, C. Di Natale, G. Bussetti, P. Chiaradia, A. Froiio, L. Valli and A. D' Amico, *Surf. Sci*., 2002, **501**, 31; c. C. Goletti, R. Paolesse, E. Dalcanale, T. Berzina, C. Di Natale, G. Bussetti, P. Chiaradia, A. Froiio, L. Cristofolini, M. Costa and A. D'Amico, *Langmuir*, 2002, **18**, 6881.
21 See, for example: (*a*) R. F. Pasternack, E. J. Gibbs, D. Bruzewicz, D. Stewart and K. S. Engstrom, *J. Am. Chem. Soc*., 2002, **124**, 3533; (*b*) R. F. Pasternack, E. J. Gibbs, P. J. Collings, J. C. dePaula, L. C. Sturzo and A. Terracina, *J. Am. Chem. Soc*., 1998, **120**, 5873.
22 (*a*) R. F. Pasternack and P. J. Collings, *Science*, 1995, **269**, 935; (*b*) R. F. Pasternack, C. Bustamante, P. J. Collings, A. Giannetto and E. J. Gibbs, *J. Am. Chem. Soc*., 1993, **115**, 5393; (*c*) J. Parkash, J. H. Robblee, J. Agnew, E. Gibbs, P. Collings, R. F. Pasternack and J. C. de Paula, *Biophys. J*., 1998, **74**, 2089.
23 (*a*) P. A. J. de Witte, M. Castriciano, J. J. L. M. Cornelissen, L Monsù Scolaro, R. J. M. Nolte and A. E. Rowan, *Chem.-Eur. J*., 2002, **9**, 1775; (*b*) P. Kubát, K. Lang, K. Procházková and P. Anzenbacher, Jr., *Langmuir*, 2003, **19**, 422.
24 K. A. Connors, *Binding Constants, The Measurement of Molecular Complex Stability*, John Wiley and Sons, New York, 1987.
25 A. P. H. J. Schenning, D. H. W. Hubert, M. C. Feiters and R. J. M. Nolte, *Langmuir*, 1996, **12**, 1572.
26 (*a*) J. C. Kemp, *J. Op. Soc. Am*., 1969, **59**, 950, see also http://www.hindspem.com; (*b*) A. Salvati and P. Chiaradia, *Appl. Opt*., 2000, **39**, 5820; (*c*) V. L. Berkovits, V. N. Bessolov, T. N. L'vova, E. B. Novikov, V. I. Safarov, R. V. Khasieva and B. V. Tsarenkov, *J. Appl. Phys*., 1991, **70**, 3707.